A Theoretical Study of Steric and Electronic Effects in the Rhodium-Catalyzed Carbonylation Reactions

Luigi Cavallo*,† and Miquel Solà‡

Contribution from the Dipartimento di Chimica, Università di Napoli, Complesso Monte S. Angelo, Via Cintia, I-80126 Napoli, Italy, and Departament de Química i Institut de Química Computacional, Universitat de Girona, 17017 Girona, Catalonia, Spain

Received June 21, 2001

Abstract: We present a QM and QM/MM study of steric and electronic effects in the main steps of Rh-catalyzed carbonylation reactions. All the considered systems adopt a square-planar geometry prior to CH_3I oxidative addition. As regards the octahedral complexes after CH_3I oxidative addition, a comparison between the various models indicates that the energy gain due to the CH_3I oxidative addition is reduced by the steric pressure of the substituents on the ligand. The substantially similar results obtained with the QM/MM and QM models indicate that electronic effects are not particularly relevant in determining the energetic of oxidative addition. As regards the **P,P-Ph** octahedral complex, the geometries in which the CO group is trans to the added CH_3 group, or trans to one of the P atoms, are of similar energy. A comparison between the various models indicates that the energy barrier of the CO insertion reaction is lowered by the presence of substituents on the chelating ligands. This effect is related to a relief of the steric pressure on the complex as the systems move from a six-coordinated octahedral geometry toward a five-coordinated square-pyramidal geometry. The energy barrier calculated for the **P,S-Ph** system is in rather good agreement with the experimental value, whereas that of the **P,P-Ph** system is somewhat underestimated. Inclusion of solvent effects with a continuum model leads to a slightly better agreement. The thermodynamic products adopt a square-pyramidal geometry with the $COCH_3$ group in the apical position.

Introduction

The migratory insertion reaction of CO into Mt−alkyl bonds is a fundamental step in many relevant organometallic reactions.[1] Among the most representative examples certainly are the rhodium-iodide catalyzed carbonylation of methanol to acetic acid and hydroformylation reactions. The original $[Rh(CO)_2I_2]^-$ catalyst, developed at the Monsanto laboratories[2,3] and studied in detail by Forster and co-workers,[4−6] is largely used for the industrial production of acetic acid and anhydride. However, the conditions used industrially (30−60 atm pressure and 150−200 °C)[7] have spurred the search for new catalysts, which could work in milder conditions.[8−17] The rate determining step of the catalytic cycle is the oxidative addition of CH_3I (see Scheme 1) so that catalyst design focused on the improvement of this reaction.

Scheme 1

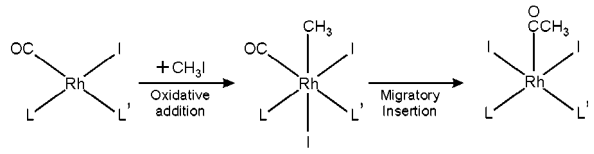

The basic idea was that ligands which increase the electron density at the metal should promote oxidative addition, and by consequence the overall rate of production. To this purpose, in the last years several other Rh compounds have been synthesized and have been demonstrated to be active catalysts of comparable or better performances compared to the original Monsanto catalyst.[8,14,18,19] One of the most important classes is based on Rh complexes containing simple phosphines such as PEt_3,[15] or biphosphine ligands of the type $PPh_2-CH_2-CH_2-PPh_2$.[13] More recently, also mixed bidentate ligands such as $PPh_2-CH_2-P(S)Ph_2$,[19] $PPh_2-CH_2-P(O)Ph_2$,[11] and $PPh_2-CH_2-P(NPh)Ph_2$[18]

† Università di Napoli.
‡ Universitat de Girona.

(1) Collman, J. P.; Hegedus, L. S.; Norton, J. R.; Finke, R. G. *Principles and Applications of Organotransition Metal Chemistry*; University Science Books: Mill Valley, CA, 1987.
(2) Robinson, K. K.; Hershman, A.; Craddock, J. H.; Roth, J. F. *J. Mol. Catal.* **1972**, *27*, 389.
(3) Paulik, F. E.; Roth, J. F. *J. Chem. Soc., Chem. Commun.* **1968**, 1578.
(4) Forster, D. *J. Am. Chem. Soc.* **1976**, *98*, 846.
(5) Forster, D. *Adv. Organomet. Chem.* **1979**, *17*, 255.
(6) Forster, D.; Singleton, T. C. *J. Mol. Catal.* **1982**, *17*, 299.
(7) Roth, J. F.; Craddock, J. H.; Hershman, A.; Paulik, F. E. *Chem. Technol.* **1971**, 600.
(8) Dilworth, J. R.; Miller, J. R.; Wheatley, N.; Baker, M. J.; Sunley, J. G. *J. Chem. Soc., Chem. Commun.* **1995**, 1579.
(9) Ghaffar, T.; Adams, H.; Maitlis, P. M.; Haynes, A.; Sunley, G. J.; Baker, M. J. *Chem. Commun.* **1998**, 1359.
(10) Haynes, A.; Mann, B. E.; Morris, G. E.; Maitlis, P. M. *J. Am. Chem. Soc.* **1993**, *115*, 4093.
(11) Wegman, R. W. *Chem. Abstr.* **1986**, *105*, 78526g.
(12) Maitlis, P. M.; Haynes, A.; Sunley, G. J.; Howard, M. J. *J. Chem. Soc., Dalton Trans.* **1996**, 2187.
(13) Moloy, K. G.; Wegman, R. W. *Organometallics* **1989**, *8*, 2883.
(14) Rankin, J.; Poole, A. D.; Benyei, A. C.; Cole-Hamilton, D. J. *Chem. Commun.* **1997**, 1835.
(15) Rankin, J.; Benyei, A. C.; Poole, A. D.; Cole-Hamilton, D. J. *J. Chem. Soc., Dalton Trans.* **1999**, 3771.
(16) Yang, J.; Haynes, A.; Maitlis, P. M. *Chem. Commun.* **1999**, 179.
(17) Gonsalvi, L.; Adams, H.; Sunley, G. J.; Ditzel, E.; Haynes, A. *J. Am. Chem. Soc.* **1999**, *121*, 11233.
(18) Katti, K. V.; Santarsiero, B. D.; Pinkerton, A. A.; Cavell, R. G. *Inorg. Chem.* **1993**, *32*, 5919.
(19) Baker, M. J.; Giles, M. F.; Orpen, A. G.; Taylor, M. J.; Watt, R. J. *J. Chem. Soc., Chem. Commun.* **1995**, 197.

10.1021/ja016468z CCC: $20.00
Published on Web 11/15/2001

have been shown to be effective catalysts. Indeed, all these new ligands enhance oxidative addition but as a consequence they usually retard the subsequent CO migratory insertion because the increased electron density at the metal also leads to a stronger Rh−CO bond. In fact, while the octahedral intermediate obtained after CH_3I addition undergoes migratory insertion only under CO pressure with PEt_3 as ligands, and it is relatively long-lived with the $PPh_2-CH_2-CH_2-PPh_2$ ligand, by contrast it is so reactive with the $PPh_2-CH_2-P(S)Ph_2$ ligand that its detection was rather difficult.[17] The fact that both oxidative addition and CO migratory insertion steps are accelerated with the latter ligand was quite unexpected, and it was hypothesized that the steric requirements of the $PPh_2-CH_2-P(S)Ph_2$ ligand destabilized the octahedral intermediate, which would undergo migratory insertion to release such steric pressure.[17]

Methanol carbonylation with the original Monsanto catalyst has been studied in detail not only experimentally[4,5,9,10,17,20,21] but also from a theoretical point of view.[20,22−25] In contrast, the same reaction promoted from phosphine-based ligands has been the subject of detailed experimental research, but not from a theoretical point of view. This is despite the potential of molecular modeling to contribute to clarify the role of steric and electronic properties of the different ligands in determining the relative rate of the two most important steps of the catalytic cycle (i.e. the oxidative addition and CO migratory insertion of Scheme 1). With the aim of filling this gap, here we present pure quantum mechanics, QM, as well as combined quantum mechanics/molecular mechanics, QM/MM, calculations on some aspects of the CH_3I oxidative addition and of the CO migratory insertion steps.

The QM approach we used is based on density functional theory, and the functional we used already has been employed by Ziegler and co-workers[22] to investigate successfully the full cycle with the Monsanto catalyst and with the new catalyst developed at BP Chemicals, in which Ir replaces Rh. Moreover, the QM/MM approach used here[26,27] is particularly useful to separate clearly between steric and electronic effects, and it has been used successfully to investigate olefin polymerizations with late transition metals,[28] with group 4 metallocenes,[29] and to clarify the origin of enantioselectivity in the chiral epoxidation of olefins with Mn-salen catalysts.[30]

To investigate the basic electronic features of the ligands, and to delay the complications of steric effects we considered the unsubstituted and simple Rh systems, including the $PH_2-CH_2-CH_2-PH_2$, $PH_2-CH_2-P(S)H_2$, $PH_2-CH_2-P(NH)H$, and $2PH_3$ as ligands, which will be referred to as **P,P**, **P,S**, **P,N**, and **2P**, respectively. However, we also performed calculations on the real-size Rh systems based on $PPh_2-CH_2-CH_2-PPh_2$, $PEt_2-CH_2-CH_2-PEt_2$, $PPh_2-CH_2-P(S)Ph_2$, $PPh_2-CH_2-P(NCH_3)Ph_2$, and $2PEt_3$ as ligands, which will be referred to in the following as **P,P-Ph**, **P,P-Et**, **P,S-Ph**, **P,N-Ph**, and **2P-Et**, respectively. To further separate between steric and electronic effects, QM/MM and pure QM calculations were performed on the real-size **P,P-Ph**, **P,P-Et**, **P,S-Ph**, **P,N-Ph**, and **2P-Et** systems.

From a comparison between the results obtained with different ligands and with different methodologies, we hope to contribute to the rationalization of the experimental results and, possibly, to furnish ideas which might be used to design new and better ligands.

Computational Details

Stationary points on the potential energy surface were calculated with the Amsterdam Density Functional (ADF) program system,[31] developed by Baerends et al.[32,33] The electronic configurations of the molecular systems were described by a triple-ζ STO basis set on rhodium for 4s, 4p, 4d, 5s, 5p and iodine for 5s, 5p (ADF basis set IV). Double-ζ STO basis sets were used for sulfur and phosphorus (3s, 3p), oxygen, nitrogen, and carbon (2s, 2p), and hydrogen (1s), augmented with a single 3d, 3d, and 2p function, respectively (ADF basis set III).[31] The inner shells on rhodium (including 3d), iodine (including 4d), sulfur and phosphorus (including 2p), and oxygen, nitrogen, and carbon (1s) were treated within the frozen core approximation. Energies and geometries were evaluated by using the local exchange-correlation potential by Vosko et al.,[34] augmented in a self-consistent manner with Becke's[35] exchange gradient correction and Perdew's[36,37] correlation gradient correction.

The ADF program was modified by one of us[27] to include standard molecular mechanics force fields in such a way that the QM and MM parts are coupled self-consistently.[26] The simple model QM systems and the full QM/MM and QM systems are displayed in Figure 1. The partitioning of the systems into QM and MM parts only involves the skeleton of the phosphine-based ligands. As for the connection between the QM and MM parts, this occurs by means of the so-called "capping" dummy hydrogen atoms, which are replaced in the real system by the corresponding "linking" carbon atom.[26,27] In the QM/MM optimizations the ratio between the C−C bonds crossing the QM/MM border and the corresponding optimized C−H distances was fixed equal to 1.26. A more detailed description of the coupling scheme, as well as further comments on the methodology, can be found in previous papers.[27,28,38] The AMBER95 force field[39] was used for the MM potentials, except for Rh and I, which were treated with the UFF force field.[40] To eliminate spurious stabilizations from the long-range attractive part of the Lennard-Jones potential,[38,41] we used an exponential expression fitted to the repulsive part of the Lennard-Jones potential.[38,42−44]

All the following structures are stationary points on the QM or combined QM/MM potential surface. Transition state geometries were approached by a linear-transit procedure, using the distance between the C(methyl) and C(CO) atoms which are going to form the new C−C bond as reaction coordinate, while optimizing all other degrees of freedom. Full transition state searches were started from geometries

(20) Griffin, T. R.; Cook, D. B.; Haynes, A.; Pearson, J. M.; Monti, D.; Morris, G. E. *J. Am. Chem. Soc.* **1996**, *118*, 3029.
(21) Dake, S. B.; Chaudhari, R. V. *J. Mol. Catal.* **1984**, *26*, 135.
(22) Cheong, M.; Schmid, R.; Ziegler, T. *Organometallics* **2000**, *19*, 1973.
(23) Kinnunen, T.; Laasonen, K. *J. Mol. Struct. (THEOCHEM)* **2001**, *540*, 91.
(24) Ivanova, E. A.; Gisdakis, P.; Nasluzov, V. A.; Rubailo, A. U.; Rösch, N. *Organometallics* **2001**, *20*, 1161.
(25) Kinnunen, T.; Laasonen, K. *J. Mol. Struct. (THEOCHEM)* **2001**, *542*, 273.
(26) Maseras, F.; Morokuma, K. *J. Comput. Chem.* **1995**, *16*, 1170.
(27) Woo, T. K.; Cavallo, L.; Ziegler, T. *Theor. Chem. Acc.* **1998**, *100*, 307.
(28) Deng, L.; Woo, T. K.; Cavallo, L.; Margl, P. M.; Ziegler, T. *J. Am. Chem. Soc.* **1997**, *119*, 6177.
(29) Guerra, G.; Longo, P.; Corradini, P.; Cavallo, L. *J. Am. Chem. Soc.* **1999**, *121*, 8651.
(30) Jacobsen, H.; Cavallo, L. *Chem. Eur. J.* **2001**, *7*, 800.
(31) ADF 2.3.0, Vrije Universiteit Amsterdam: Amsterdam, The Netherlands, 1996.
(32) Baerends, E. J.; Ellis, D. E.; Ros, P. *Chem. Phys.* **1973**, *2*, 41.
(33) te Velde, G.; Baerends, E. J. *J. Comput. Phys.* **1992**, *99*, 84.
(34) Vosko, S. H.; Wilk, L.; Nusair, M. *Can. J. Phys.* **1980**, *58*, 1200.
(35) Becke, A. *Phys. Rev. A* **1988**, *38*, 3098.
(36) Perdew, J. P. *Phys. Rev. B* **1986**, *33*, 8822.
(37) Perdew, J. P. *Phys. Rev. B* **1986**, *34*, 7406.
(38) Cavallo, L.; Woo, T. K.; Ziegler, T. *Can. J. Chem.* **1998**, *76*, 1457.
(39) Cornell, W. D.; Cieplak, P.; Bayly, C. I.; Gould, I. R.; Merz, K. M. J.; Ferguson, D. M.; Spellmeyer, D. C.; Fox, T.; Caldwell, J. W.; Kolmann, P. A. *J. Am. Chem. Soc.* **1995**, *117*, 5179.
(40) Rappé, A. K.; Casewit, C. J.; Colwell, K. S.; Goddard, W. A., III; Shiff, W. M. *J. Am. Chem. Soc.* **1992**, *114*, 10024.
(41) Sauers, R. R. *J. Chem. Educ.* **1996**, *73*, 1996.
(42) Lee, K. J.; Brown, T. L. *Inorg. Chem.* **1992**, *31*, 289.
(43) Woo, T. K.; Ziegler, T. *Inorg. Chem.* **1994**, *33*, 1857.
(44) Guerra, G.; Cavallo, L.; Corradini, P.; Longo, P.; Resconi, L. *J. Am. Chem. Soc.* **1997**, *119*, 4394.

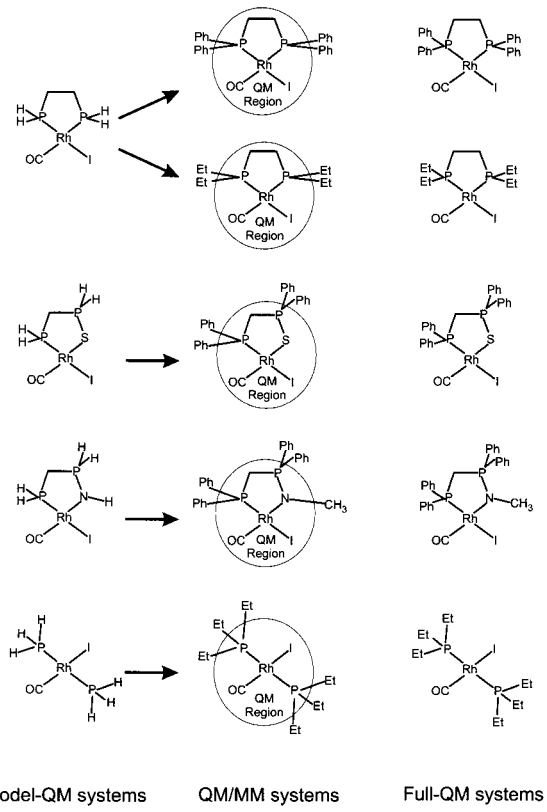

Figure 1. Representation of the scheme used to partition the various QM/MM systems into the QM and MM regions, respectively.

corresponding to maxima along the linear-transit curves. At the end of each transition state search, the real nature of the transition states was checked with frequency calculations, which resulted in only one imaginary frequency. This check was performed on the transition states of the unsubstituted QM P,P, P,S, P,N, and 2P simple models, and on the full systems at the QM/MM level of theory. Pure QM frequency calculations were not performed on the full systems due to the large number of atoms considered, and to the strong similarity between the QM/MM and QM calculations on the full systems.

Energy differences with inclusion of solvent effects were calculated by correcting the gas-phase energy with the use of the conductor-like screening model, COSMO, of Klamt and Schüürmann,[45] as implemented in the ADF package.[46] The calculations of the solvation energy were performed with a dielectric costant of 8.39 to represent CH_2Cl_2 as solvent. The van der Waals surface was used to build the cavity containing the molecule, and the standard radii (Å) [H = 1.29, C = 2.00, N = 1.83, O = 1.71, P = 2.10, S = 2.16, and I = 2.31] of Klamt and Schüürmann were used.[45] For Rh, we used a radius of 2.30 Å. The calculations of energies including solvation effects were performed as single-point calculations on the gas-phase optimized geometries. The 2000.01 release of the ADF package was used for these calculations.[47]

Results and Discussion

The Square-Planar Precursors. The geometries of the most stable square-planar complexes prior to oxidative addition of CH_3I are reported in Figure 2.

The effects of steric and electronic properties of the different ligands can be obtained from a comparison of the different structures. First, the inclusion of the Ph or Et substituents on the model QM systems **P,P**, **P,S**, **P,N**, and **2P** pushes the P, S, and N atoms of the ligands away from the metal. This effect is

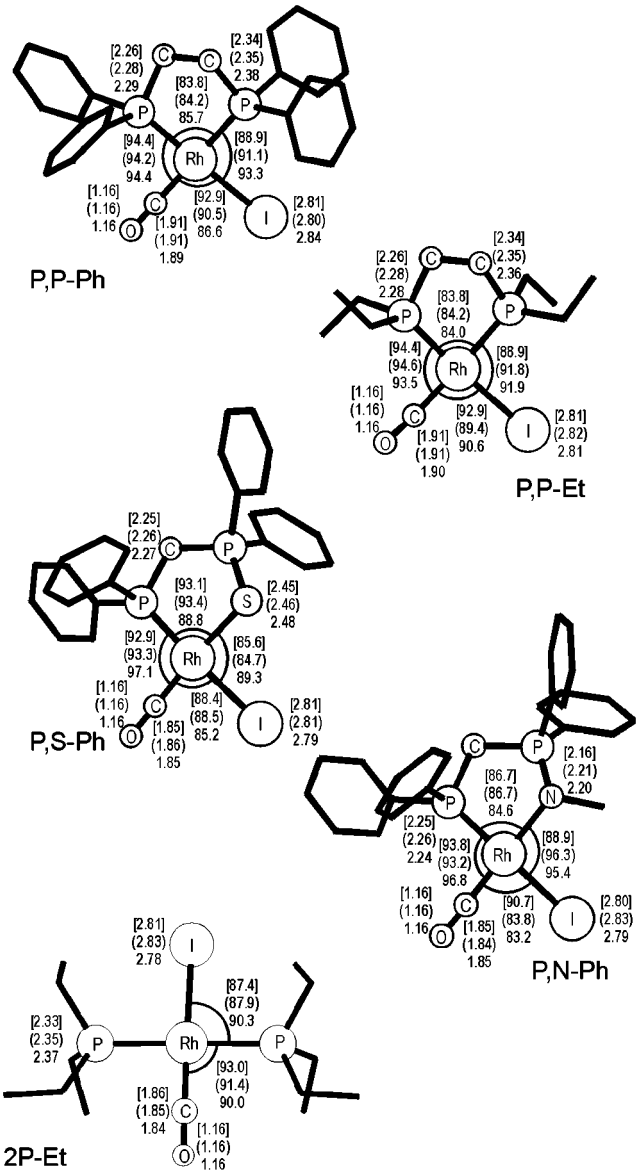

Figure 2. Minimum energy geometries of the square-planar complexes before CH_3I addition. Distances and angles are in Å and deg, respectively. The unbracketed values refer to the "real-size" full-QM geometry, while the round- and square-bracketed values refer to the "real-size" QM/MM and unsubstituted model-QM geometries, respectively.

smaller in the **P,P-Et** and **2P-Et** systems, because of the smaller steric requirements of the Et groups compared to the Ph groups. Longer Rh−P distances in the full **P,P-Ph** systems (QM/MM and pure QM) relative to the model **P,P** system correspond to shorter Rh−CO distances, as a consequence of the smaller trans effect of the P atom that is trans to the CO group. Finally, it is worth noting that the Rh−CO bond length is roughly 0.05 Å shorter in the **P,S-Ph** and **P,N-Ph** systems, relative to the same distance in the model **P,P** systems. This is a consequence of the π-donating properties of the S and N atoms, which lead to more pronounced d−π* Rh-to-CO back-donation. This is suggested also by the slightly longer C−O bond distance in the model **P,S** system relative to the same distance in the model **P,P** system (1.152 and 1.149 Å, respectively), and by the slightly lower C−O frequency in the QM/MM **P,S-Ph** system relative to the same frequency in the QM/MM **P,P-Ph** system (1986 and 1999 cm^{-1}, respectively). These results are in agreement with the lower CO frequency for the **P,S-Ph** system compared

(45) Klamt, A.; Schüürmann, G. *J. Chem. Soc., Perkin Trans. 2* **1993**, 799.
(46) Pye, C. C.; Ziegler, T. *Theor. Chem. Acc.* **1999**, *101*, 396.
(47) ADF 2000, Vrije Universiteit Amsterdam: Amsterdam, The Netherlands, 2000.

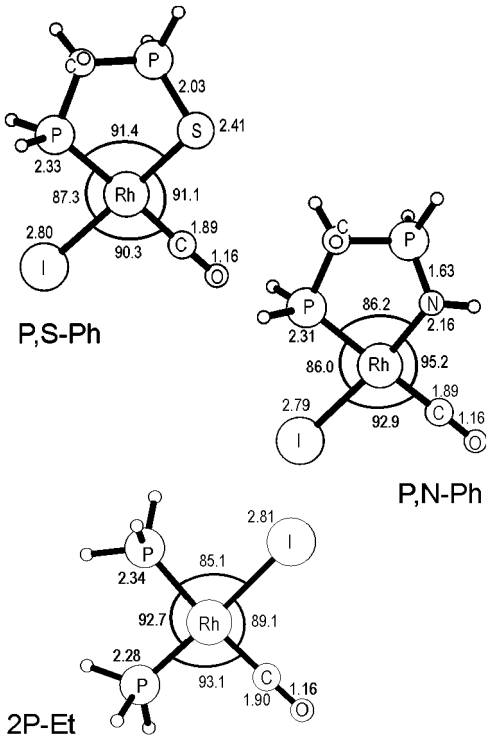

Figure 3. Minimum energy geometries of the unsubstituted model-QM geometries of the square-planar complexes before CH_3I addition, in which the CO group is trans to the P atom. Distances and angles are in Å and deg, respectively.

to the **P,P-Ph** system observed experimentally by Haynes and co-workers (1987 and 2011 cm^{-1}, respectively).[17]

As regards the angles, the I−Rh−CO angle is reduced by roughly 5° for all the systems, which is different from the effect of the substituents on the other bend angles around the metal. In case of the **P,P** system, the inclusion of the Ph substituents opens the P−Rh−I substantially, to reduce steric interactions between the I^- ligand and the Ph groups; however, the P−Rh−CO angle remains substantially unchanged due the smaller dimensions of the CO ligand relative to the I^- ligand. The P−Rh−P angle also remains substantially unchanged. The effect of the Ph substituents on the **P,S** and **P,N** systems is quite different. In these cases, the most severe repulsive interactions occur between the Ph groups bonded to the P atom coordinated to the metal and the CO group. To relieve these interactions, the P−Rh−C angles open up 4° roughly. In a concerted way, the P−Rh−S and P−Rh−N angles are reduced. The geometry of the **P,S-Ph** system can be compared with the X-ray structure of the analogous $[Rh(CO)Cl(PPh_2CH_2PPh_2S)]$ compound. The distances of coordination around the Rh atom in the **P,S-Ph** full QM structure slightly overestimate the experimental values of the Rh−C, Rh−P, and Rh−S distances, 1.83, 2.22, and 2.40 Å, respectively, found in the X-ray structure of this compound by Baker and co-workers.[19]

Finally, test calculations on the simplified QM model also indicated that for the model **P,S** and **P,N** ligands, the geometry with the CO trans to the S or N atom is favored energetically relative to the geometry with the CO trans to the P atom, and reported in Figure 3, by 25 and 48 kJ/mol for the **P,S** and **P,N** ligands, respectively. The electronic preference for geometries with CO trans to S or N can be explained by the π-electron donating properties of S and N, which improve metal-to-CO back-donation. On the basis of the above, in the remainder of this paper we only considered geometries in which the CO ligand is trans to the S or N atom. For the **2P** system, instead,

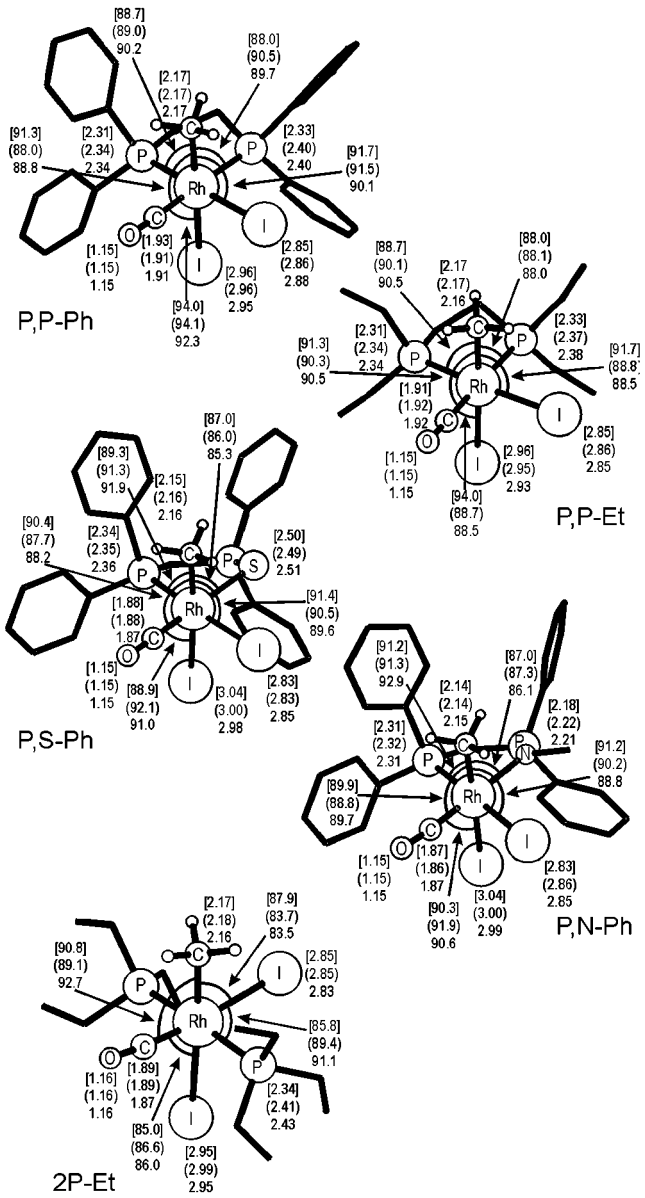

Figure 4. Minimum energy geometries of the octahedral complexes after CH_3I addition. Distances and angles are in Å and deg, respectively. The unbracketed values refer to the "real-size" full-QM geometry, while the round- and square-bracketed values refer to the "real-size" QM/MM and unsubstituted model-QM geometries, respectively.

the geometry of the square-planar Vaska-type precursor in which the two PH_3 ligands are cis to each other is less stable by 27 kJ/mol, relative to the trans disposition of the two PH_3 ligands. This preference is in agreement with previous calculations by Ziegler and co-workers on the $Rh(PH_3)_2ClCO$ complex,[48] and by Morokuma and co-workers on the $Rh(PH_3)_2HCO$ and $Rh(PH_3)_2(CO)(C(=O)C_2H_5)$ complexes.[49] In these cases, the trans geometry was favored by 37, 13, and 22 kJ/mol, respectively. The higher stability of the trans geometry can be explained by the relative strength of CO, PH_3, and I^- as trans-destabilizing ligands with CO > $PH_3 \gg I^-$.

The Octahedral Intermediates. The geometries of the octahedral complexes, after oxidative addition of CH_3I to the square-planar complexes of Figure 2, are reported in Figure 4.

(48) Margl, P.; Ziegler, T.; Blöchl, P. E. *J. Am. Chem. Soc.* **1995**, *117*, 12625.

(49) Matsubara, T.; Koga, N.; Ding, Y.; Musaev, D. G.; Morokuma, K. *Organometallics* **1997**, *16*, 1065.

The methyl group is in an axial position.[50] After CH_3I addition, the distances of the P, S, CO, and I^- from Rh are considerably elongated. This feature is observed in all the models, and thus sterics do not play a role in this effect, which is only electronic in nature.

The main geometric deformations due to the presence of the substituents on the **P,P**, **P,S**, **P,N**, and **2P** systems are quite similar to those already observed in the square-planar complexes. Of interest are the effects of the substituents on the position of the added CH_3 group. In the case of **P,P-Ph**, according to pure QM calculations on the full system the greatest deviation from 90° amounts to 1.2°, and corresponds to the angle $CH_3-Rh-CO$. All the other CH_3-Rh-X angles (X is a substituent in the equatorial plane) are considerably close to 90°. The $Rh-CH_3$ and Rh−CO bond lengths are roughly 0.02 and 0.04 Å shorter in the **P,S-Ph** systems relative to the same distance in the model **P,P** systems. The QM/MM energy required to dissociate the CO molecule from the equatorial plane is predicted to be substantially higher for the **P,S-Ph** system than for the **P,P-Ph** system, 151 vs 121 kJ/mol, respectively. This is a consequence of the electron-donating properties of the S atom, which increase the electron density at the metal and as a consequence the Rh-to-CO back-donantion.

Quite different, instead, is the geometry around the Rh atom in the case of the **P,S-Ph** and **P,N-Ph** ligands. For these systems, according to pure QM calculations on the real-size systems, the $P-Rh-CH_3$ angle is larger than 90° by 2−3°, while the $S-Rh-CH_3$ and $N-Rh-CH_3$ angles are close to 85°. The origin of this effect is clearly steric in nature, since these deviations are absent in case of the unsubstituted model **P,S** and **P,N** systems. Similar deformations were observed by Haynes and co-workers in the X-ray structure of the strictly related Ir compound $[CH_3Ir(CO)I_2(PPh_2CH_2PPh_2S)]$, which is the same **P,S-Ph** complex we investigated where an Ir atom replaces the Rh atom.[17] In the crystalline structure, the $P-Ir-CH_3$ and $S-Ir-CH_3$ angles are equal to 96.4° and 86.3°, respectively. However, both in our calculations as well as in the crystalline structure, the methyl group is pushed toward the less encumbered quadrant defined by the S and I atoms. In fact, the CH_3-Rh-I angle is slightly smaller than 90°, by roughly 1−2°, according to the crystalline structure and to our calculations, and this occurs for all the systems considered here. The $CH_3-Rh-CO$ angle is reduced slightly by the inclusion of the various substituents, and to this small reduction of the $CH_3-Rh-CO$ angle corresponds a small decrease, roughly 0.05 Å, of the distance between the C atoms of the CH_3 and CO groups. Again, this is not peculiar of the P,S based systems but it is calculated for all the systems considered in this paper. As regards the 2P systems, they retain a substantial regular octahedral geometry around the metal, since only the I−Rh−I angle deviates from 90° in a substantial way. The distances of coordination around the Rh atom in both the **2P-Et** QM/MM and full QM structures slightly overestimate the experimental values of the $Rh-CH_3$, Rh−CO, Rh−P, Rh−I (trans to CO), and Rh−I (trans to CH_3) distances, 2.11, 1.84, 2.39, 2.72, and 2.78 Å, respectively, found in the X-ray structure of this compound by Cole−Hamilton and co-workers.[14,15]

For a better comparison with X-ray determined structures, the superposition of the **P,P-Ph** full QM model with the crystal structure of the related $[IrI_4(PPh_2CH_2CH_2PPh_2)]^-$ anion[51] and that of the **P,S-Ph** full QM model with the crystal structure of $[CH_3Ir(CO)I_2(PPh_2CH_2PPh_2S)]$[17] are reported in Figure 5. In both cases, the superposition has been performed on the metal and on the six atoms coordinated to it. The sketches clearly indicate that the ligand conformation of our **P,P-Ph** geometry looks very similar to the crystal structure, whereas our **P,S-Ph** geometry does not mimic the crystal structure very well. In both P,S-based structures, the five-membered chelate ring adopts an envelope-like conformation, but in the X-ray structure the C atom is at the apex of the envelope, while in the QM structure the Rh atom is at the apex.

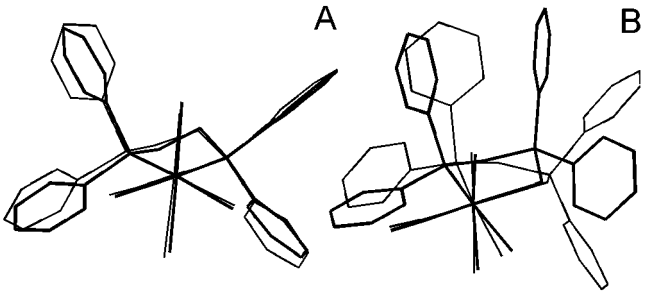

Figure 5. Schematic superposition of the full QM structure **P,P-Ph**, part A, and **P,S-Ph**, part B, with the crystal structure of the $[IrI_4(PPh_2CH_2CH_2PPh_2)]^-$ anion and of the $[CH_3Ir(CO)I_2(PPh_2CH_2PPh_2S)]$ compund, respectively. Thin and bold lines correspond to the calculated and the X-ray structures, respectively.

This similarity between the calculated and the X-ray structures of the P,P based systems, as well as the discrepancy in the case of the P,S based ones, holds also for the acetyl products which will be discussed later. However, in all the P,S based crystal structures two of the phenyl groups adopt a parallel orientation with a mean distance between the two planes of roughly 3.5−4.0 Å.[17,19,52] This suggests that $\pi-\pi$ stacking interactions could stabilize this conformation in the crystals. Incidentally, this effect has been proposed to be at the origin of geometrical distortions in Pd compunds.[53,54] This stabilizing effect, if present, should be of minor relevance in solvents of relatively high polarity such as CH_2Cl_2 due to attractive halogen−aromatic ring interactions.[55,56] According to our calculations, the QM/MM and full QM structure of the octahedral **P,S-Ph** complex with a conformation similar to that of the crystal structure are 17 and 14 kJ/mol higher in energy, relative to the minimum energy structure of Figures 4 and 5.

However, we also considered situations in which the CO group is trans to the CH_3 group, since this geometry was experimentally found by Moloy and Wegman for the **P,P-Ph** system.[13] Thus, we confined the analysis to the **P,P-Ph** system and, for comparison, to the **P,S-Ph** system. The corresponding geometries are reported in Figure 6. Aside from the geometrical deformations due to the inclusion of the Ph substituents, the most noticeable features are the shortening of the Rh−I bond that moved from the axial position, where it experienced the trans properties of the CH_3 group, and the corresponding elongation of the Rh−CO bond. A decreased back-donation to the CO π^* orbital, which results in a shortening of the CO bond, corresponds to the longer Rh−CO bond. As for energetics, the

(50) For the sake of simplicity, throughout this work we define the plane containing the Rh atom and the two chelating atoms of the P,P, P,S and P,N based systems as the equatorial plane. The axial and equatorial notations thus refer to the coordination positions perpendicular to or lying in the equatorial plane, respectively.

(51) Ng Cheong Chan, Y.; Meyer, D.; Osborn, J. A. *J. Chem. Soc., Chem. Commun.* **1990**, 869.
(52) Wong, T. Y. H.; Rettig, S. J.; James, B. R. *Inorg. Chem.* **1999**, *38*, 2143.
(53) Drago, D.; Pregosin, P. S.; Tschperner, M.; Albinati, A. *J. Chem. Soc., Dalton Trans.* **1999**, 2279.
(54) Magistrato, A.; Merlin, M.; Pregosin, P. S.; Rothlisberger, U.; Albinati, A. *Organometallics* **2000**, *19*, 3591.
(55) Hobza, P.; Selzle, H. L.; Schlag, E. W. *Chem. Rev.* **1994**, *94*, 1767.
(56) Neusser, H. J.; Krause, H. *Chem. Rev.* **1994**, *94*, 1829.

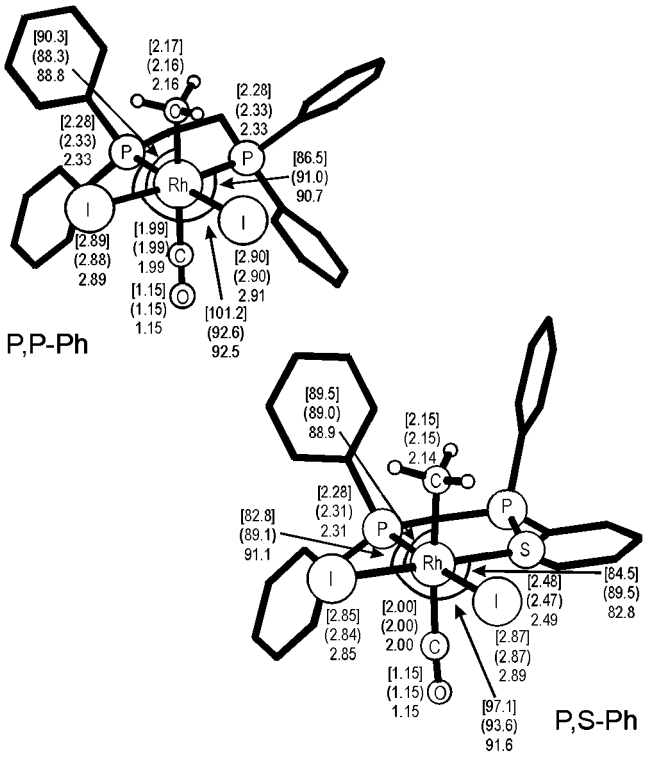

Figure 6. Minimum energy geometries of the octahedral complexes with the CO group trans to the CH_3 group. Distances and angles are in Å and deg, respectively. The unbracketed values refer to the "real-size" full-QM geometry, while the round- and square-bracketed values refer to the "real-size" QM/MM and unsubstituted model-QM geometries, respectively.

P,P QM and **P,P-Ph** QM/MM systems with CO trans to the CH_3 group are 16 and 17 kJ/mol higher in energy with respect to the corresponding systems with the CO in the equatorial plane. However, in the case of pure QM calculations on the **P,P-Ph** system, we found that the geometry with the CO trans to the CH_3 group is slightly more stable, by 1 kJ/mol only, than the corresponding systems with the CO in the equatorial plane. These results clearly indicate that we are in the presence of electronic effects only. The acidity of the Ph-substituted phosphorus reduces the density at the metal atom, and hence it destabilizes a trans π*-acceptor ligand, such as CO, and stabilizes a trans π-electron donating ligand such as I^-. On the other hand, in case of the **P,S-Ph** system, the Ph substituents substantially have no effects, since they are not bonded to the S atom which is, on the other hand, an electron-donating atom. For this reason, in the case of the P,S based systems, geometries with the CO ligand in the equatorial plane, and trans to the S atom, are favored with respect to the same geometries with the CO ligand in the axial position by 35, 40, and 30 kJ/mol, in the model **P,S** and in the QM/MM and pure QM **P,S-Ph** systems, respectively.

The Transition States. The geometries of the transition states of the CO migratory insertion are reported in Figure 7. In all cases the CH_3 bends toward the CO group to form the new C−C bond. Aside of the reacting groups the major differences between the octahedral complexes and the transition states is the elongation of the Rh−X bond trans to the CO in the octahedral complex. This elongation is smaller for **P,P-Ph**, although it is quite clear when the simple **P,P** system or the **P,P-Et** system with the smaller Et substituents are considered. Instead, it is rather strong when the **P,S-Ph**, **P,N-Ph**, and **2P-Et** systems, as well as the **P,S**, **P,N**, and **2P** systems, are considered. In these cases the elongation of the Rh−S, Rh−N, and Rh−I distances is close to 0.15 Å. As pointed out by Ziegler and co-workers this is the result of the trans effect of the forming acyl group, and it is stronger for the most electron-rich P,S and P,N based systems, and for the system with the soft I^- ligand trans to the forming acyl group.[22] To decrease this trans effect, the CO group moves out of the equatorial plane more in the P,S and P,N based systems than in the P,P based systems, as suggested by the OC−Rh−S and OC−Rh−N angles which deviate by roughly 30° from 180°, while the corresponding OC−Rh−P angle deviates roughly 20° only. As a consequence, in the P,S and P,N based systems the methyl group is bent toward the atom trans to the CO, as indicated by the S−Rh−CH_3 and N−Rh−CH_3 angles close to 100°. In all the P,P based systems, the corresponding CH_3−Rh−P angle is roughly 10° wider. To the Rh−S and Rh−N elongation corresponds a shortening of

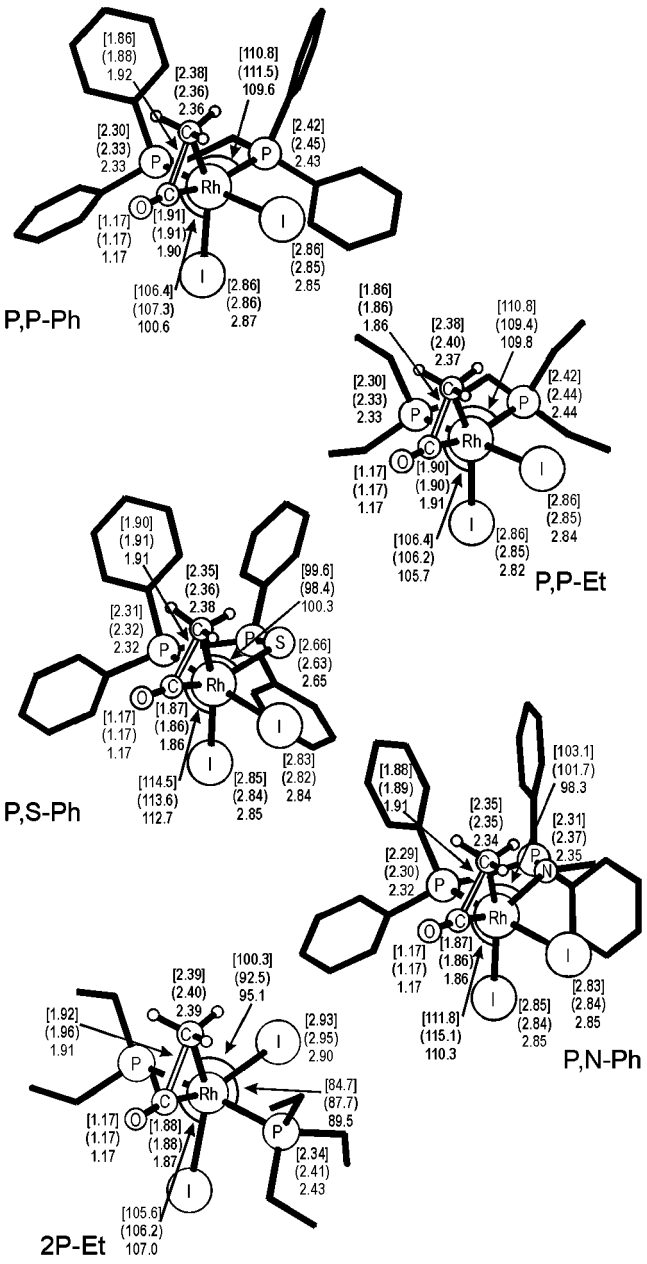

Figure 7. Geometries of the transition states of the CO insertion reaction. Distances and angles are in Å and deg, respectively. The unbracketed values refer to the "real-size" full-QM geometry, while the round- and square-bracketed values refer to the "real-size" QM/MM and unsubstituted model-QM geometries, respectively.

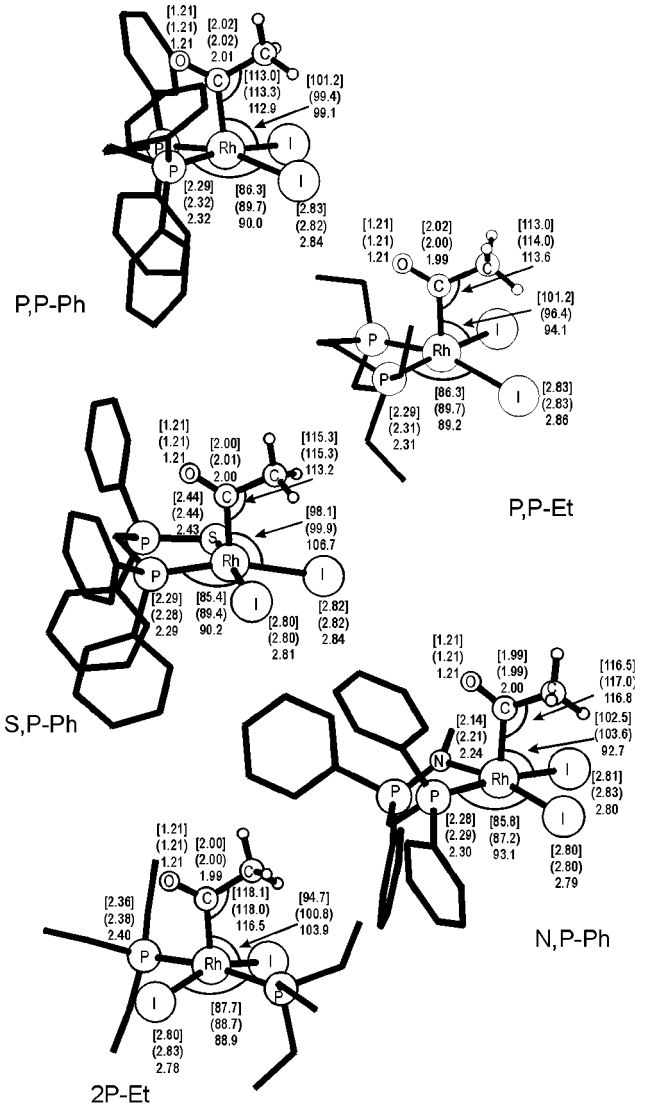

Figure 8. Minimum energy geometries of the square-pyramidal products after CO insertion. Distances and angles are in Å and deg, respectively. The unbracketed values refer to the "real-size" full-QM geometry, while the round- and square-bracketed values refer to the "real-size" QM/MM and unsubstituted model-QM geometries, respectively.

the P═S and P═N bonds from 2.03 and 1.63 Å in the octahedral complexes to 2.01 and 1.61 Å in the transition states, respectively.

Quite remarkable also is the effect of the Ph substituents on the position of the transition state along the reaction coordinate in the case of the **P,P** systems. In fact, the forming C−C bond is longer by 0.06 Å in the full **P,P-Ph** system than in the model **P,P** system. In all the other systems considered, the length of the forming C−C bond is substantially the same on going from the model QM systems to the QM/MM systems to the full QM sytems. In the case of the **P,P-Ph** system, instead, the steric and electronic properties of the flanking Ph groups favor the migratory insertion of the CO group, and the transition state is reached earlier with respect to the model **P,P** system.

The Thermodynamic Products. The geometries of the thermodynamic products after CO migratory insertion are reported in Figure 8.

In agreement with previous calculations on similar carbonylation systems,[22] the thermodynamic product corresponds to a square pyramid with the formed acyl group in the apical position. In all the systems with a chelating ligand the lowest energy situation corresponds to the geometry in which the C═O bond of the acyl group is oriented toward the bridge of the chelating ligand. There is no evidence of agostic interactions between the acylic CH_3 group and the metal. All the distances of the P, S, N, and I atoms from the metal center are roughly 0.05 Å shorter with respect to octahedral complexes of Figure 4, and are even slighlty shorter with respect to analogous distances in the square-planar complexes of Figure 1. The Rh−C(acyl) distance is close to 2.0 Å, which has to be compared with the values of roughly 1.9 and 2.2 Å, assumed by the Rh−C(CO) and Rh−C(CH_3) distances in the octahedral complexes. The main differences between the unsubstituted QM model systems and the QMMM and full QM models substantially are analogous to those previously described for the octahedral complexes, and hence are not discussed. In the case of the **P,S-Ph** systems the distances of coordination around the Rh atom slightly overestimate the experimental values of the Rh−C, Rh−P, Rh−S, Rh−I (trans to P), and Rh−I (trans to S) distances, 1.95, 2.26, 2.36, 2.70, and 2.65 Å, respectively, found in the X-ray structure of this compound by Haynes and co-workers.[17] Inclusion of relativistic effects in the geometry optimizations would probably reduce slightly the Rh-ligands distances, and thus would lead to a better agreement with the X-ray structures.

Table 1. Energies of the Square Planar (SP Complex) and Free CH_3I Reactants, of the Octahedral Intermediates (Oh Complex), of the Transition States and of the Thermodynamic Products of the CO Insertion into the Rh−CH_3 Bond[a]

		Δ*E* (kJ/mol)			
ligand	geometry	SP complex + CH_3I	Oh complex	transition state	products
		model-QM systems			
P,P	CO trans to P	64	0	82	−40
P,P	CO trans to CH_3		16		
P,S	CO trans to S	56	0	74	−36
P,S	CO trans to P	81			
P,S	CO trans to CH_3		35		
P,N	CO trans to N	64	0	82	−21
P,N	CO trans to P	112			
2P	CO trans to I^-	43	0	66	−38
2P	CO trans to P	70			
		"real-size" QM/MM systems			
P,P-Ph	CO trans to P	43	0	73	−47
P,P-Ph	CO trans to CH_3		17		
P,P-Et	CO trans to P	50	0	73	−43
P,S-Ph	CO trans to S	43	0	67	−38
P,S-Ph	CO trans to CH_3		40		
P,N-Ph	CO trans to N	46	0	72	−15
2P-Et	CO trans to I^-	35	0	79	−36
		"real-size" full-QM systems			
P,P-Ph	CO trans to P	43	0	61	−57
P,P-Ph	CO trans to CH_3		−1		
P,P-Et	CO trans to P	60	0	85	−18
P,S-Ph	CO trans to S	41	0	56	−56
P,S-Ph	CO trans to CH_3		30		
P,N-Ph	CO trans to N	55	0	70	8
2P-Et	CO trans to I^-	40	0	78	−12
		"real-size" full-QM + COSMO ($\epsilon = 8.93$) systems			
P,P-Ph	CO trans to P	55	0	70	−48
P,P-Et	CO trans to P	67	0	84	−30
P,S-Ph	CO trans to S	44	0	56	−57
P,N-Ph	CO trans to N	54	0	77	11
2P-Et	CO trans to I^-	48	0	78	−3

[a] For each system, the octahedral intermediate is assumed as reference geometry at zero energy.

Discussion. The relative energies of all the structures discussed so far are reported in Table 1.

As regards the model **P,P**, **P,S**, **P,N**, and **2P** systems, the CH_3I oxidative addition to the square-planar precursors is exothermic by 64, 56, 64, and 43 kJ/mol, respectively. Addition of the Ph or Et substituents on the various model systems has a remarkable effect on the enthalpy of oxidative addition, since the steric pressure of the substituents strongly destabilizes the octahedral complexes relative to the square-planar complexes. The most dramatic effect is for the **P,P-Ph** and **P,N-Ph** systems, whose enthalpies of oxidative addition decrease by 21 and 18 kJ/mol, with the QM/MM models, with respect to that of the model **P,P** and **P,N** systems. Relevant, although smaller, are steric effects on the **P,P-Et**, **P,S-Ph**, and **2P-Et** systems, whose energies of oxidative addition decrease by 14, 13, and 8 kJ/mol, with the QM/MM models, with respect to that of the model **P,P**, **P,S**, and **2P** systems. The major effects observed for the **P,P-Ph** and **P,N-Ph** systems can be ascribed to the four Ph groups flanking the axial CH_3 and I^- substituents in the case of the **P,P-Ph** system, and of the combined effect of the Ph groups on the P atom, and of the methyl group on the N atom, which reduces the flexibility of the **P,N** ligand, through repulsive interaction between this methyl group and the I^- ligand in the equatorial plane. The results obtained with the relatively simple QM/MM approach are substantially confirmed when pure QM calculations are performed on the full systems. The Ph groups destabilize the **P,P-Ph** and **P,S-Ph** octahedral complexes by 21 and 15 kJ/mol, respectively, while the effect of the substituents on the **P,P-Et**, **P,N-Ph**, and **2P-Et** systems is reduced, since the relative octahedral complexes are destabilized by 4, 9, and 3 kJ/mol, respectively. These values can be compared with the value of 23−35 kJ/mol (depending on the particular geometry of the resulting octahedral intermediate) predicted for the oxidative addition of CH_3I to $[(CO)_2RhI_2]^-$ by Ivanova et al.[24] As expected, and in qualitative agreement with the experimental results, the oxidative additions in all the systems we considered are considerably more exothermic than those predicted by Ivanova et al.

Inclusion of solvent effects slighlty changes the value of the energy of CH_3I oxidative addition. The systems most affected are the **P,P-Ph**, **P,P-Et**, and **2P-Et** systems, since inclusion of solvent effects in these systems favors oxidative addition by roughly 10 kJ/mol relative to the gas-phase values. As regards the **P,S-Ph** and **P,N-Ph** systems, the gas-phase and solution values are substantially the same. The slightly higher values of the energy of the CH_3I oxidative addition in solution for the former systems is essentially due to a greater increase in the dipole moment, roughly 1 D, on going from the square-planar to the octahedral complexes.

With regard to the energy barrier of the CO migratory insertion, for the model **P,P**, **P,S**, **P,N**, and **2P** systems we calculated energetic barriers of 82, 74, 82, and 66 kJ/mol. The lower energy barrier corresponds to the **2P** system, while for a comparison between the **P,P** and **P,S** systems, the energy barrier of the latter is lower by 8 kJ/mol. Inclusion of the Ph or Et substituents substantially lowers the barrier to CO migratory insertion of roughly 10 kJ/mol in all cases, with the exception of the **2P-Et** system. The smaller barrier calculated with the QM/MM models is substantially due to a relief of the steric pressure in the octahedral complex, as the systems move toward the square-pyramidal products. More remarkable are the effects of the substituents on the energetic barrier to CO insertion when the full systems are calculated with pure QM methods. In fact, when Ph substituents are considered, the barrier is lowered by 21, 18, and 12 kJ/mol for the **P,P-Ph**, **P,S-Ph**, and **P,N-Ph** systems, respectively. For the **P,P-Et** and **2P-Et** systems, instead, the energetic barrier is increased by 3 and 12 kJ/mol relative to the model **P,P** and **2P** systems. Such sharp differences between the QM/MM and the QM calculations on the full systems can be ascribed to electronic effects only. As correctly suggested by Ziegler, Haynes, and relative co-workers in previous papers,[17,22] electron-attractive groups favor the migratory insertion reaction by reducing the electron density on the metal and, as a consequence, by decreasing the strength of the $Rh-CH_3$ bond. On the contrary, electron-donating groups, as the Et substituents on the **P,P-Et** and **2P-Et** systems, normally retard CO insertion.

The values we calculated for the migratory insertion barrier can be compared with the values of 73 and 76 kJ/mol calculated for the same reaction in the $[(CO)_2RhI_3CH_3]^{2-}$ system by Ziegler and co-workers[22] and Ivanova et al.,[24] respectively. The migratory insertion barrier we calculated for the full QM **P,P-Ph** system, and particularly for the **P,S-Ph** system, is clearly lower than those calculated for the $[(CO)_2RhI_3CH_3]^{2-}$ system, which is consistent with the high migratory insertion rate experimentally shown by the **P,S-Ph** system.[17]

Inclusion of solvent effects does not change substantially the value of the CO insertion barriers. In fact, the barriers of **P,P-Et**, **P,S-Ph**, and **2P-Et** are substantially the same after inclusion of solvent effects, while the barriers of **P,P-Ph** and **P,N-Ph** are slightly increased by about 5−10 kJ/mol relative to the gas-phase values.

The relative ordering of the CO insertion barriers we calculated is in rather good agreement with the experimental reactivity. In fact, the system based on the **P,S-Ph** complex, for which we calculated the smallest barrier, is the one that gives the fastest CO insertion experimentally, while the system based on the **2P-Et** complex, for which we calculated a relatively high barrier, gives CO insertion only under CO pressure experimentally. Moreover, the barrier we calculated for the **P,S-Ph** system, 56 kJ/mol both in the gas-phase and in solution, is in good agreement with the experimental $\Delta H^{\ddagger}$ value of 54 ± 7 kJ/mol. Instead, the barrier to CO insertion we calculated for the **P,P-Ph** system, 61 and 70 kJ/mol in the gas phase and in solution, respectively, clearly underestimates the experimental value of 83 ± 2 kJ/mol. Since the COSMO model accounts for electrostatic effects only, we decided to perform test calculations on the **P,P-Ph** and **P,S-Ph** systems with the PCM approach,[57−59] which includes also nonelectrostatic terms, cavitation, and van der Waals, specifically, to the solvation energy. However, also this approach does not lead to a better agreement with experiments, since the gas-phase barriers of both the **P,P-Ph** and **P,S-Ph** systems are slightly reduced, by 2 and 1 kJ/mol, respectively. Considering the rather good agreement we found for the case of the **P,S-Ph** system, is difficult to rationalize the discrepancy between experimental and calculated CO insertion barriers in the case of the **P,P-Ph** system, although a failure of our computational approach (the particular density functional we used, zero-point energy corrections, relativistic effects, for example) always has to be considered.

First, it could be given to specific interactions of the system with solvent molecules, an hypothesis already utilized by Ziegler and co-workers when comparing the experimental and theoretical CO insertion barriers in the $[Mt(CO)_2I_2]^-$ (Mt = Rh, Ir) systems.[22] In this respect, specific solvent effects through $C-H\cdots\pi$ interactions are well-known.[60,61] According to the

(57) Miertus, S.; Scrocco, E.; Tomasi, J. *J. Chem. Phys.* **1981**, *55*, 117.
(58) Tomasi, J.; Persico, M. *Chem. Rev.* **1994**, *94*, 2027.
(59) Orozco, M.; Luque, F. J. *Chem. Rev.* **2000**, *100*, 4187.
(60) Hobza, P.; Spirko, V.; Selzle, H. L.; Schlag, E. W. *J. Phys. Chem. A* **1998**, *102*, 2501.

calculations by Luque et al., the complex $CH_4\cdots C_6H_6$ is stabilized by 6 kJ/mol through $C-H\cdots\pi$ interactions and the $CHCl_3\cdots C_6H_6$ complex is stabilized by 26 kJ/mol.[61] A $C-H\cdots\pi$ interaction of the phenyl rings in our complex with the CH_2Cl_2 solvent should involve a stabilization energy of something intermediate between 6 and 26 kJ/mol. This hypothesis originates from a small reduction, roughly 15 Å^2, in the solvent accessible surface area of the **P,P-Ph** system, on going from the octahedral complex to the transition state. This could imply reduced favorable interactions with solvent molecules in the transition state. For the **P,S-Ph** system, instead, the solvent-accessible surface area of the transition state is substantially identical with that of the octahedral complex.

As an alternative, considering the almost identical energy of the geometries of the octahedral **P,P-Ph** complex in which the CO is cis or trans to the CH_3 group, it could be possible that a sizable amount of the complex could assume a geometry with the CO trans to the CH_3 group (this structure is not suitable to give CO insertion). Clearly, this could affect the measure of the experimental $\Delta H^{\ddagger}$ of CO insertion if a fast equilibrium between the two isomers is not reached. These two isomers were experimentally found by Moloy and Wegman,[13] and were clearly distinguishable in the ^{1}H and ^{31}P NMR spectra, although the IR shows a single ν(CO) band at 2065 cm^{-1}. The frequency of this band in the mechanistic study of Moloy and Wegman is in good agreement with the value of 2062 cm^{-1} found by Haynes and co-workers in their kinetic study.[17] For the sake of completeness, the QM/MM frequency calculations we performed for the two isomers resulted in similar but not identical CO frequencies at 2029 and 2043 cm^{-1} for the isomers with the CO group trans or cis to the CH_3 group, respectively.

Finally, as regards the energetics of the migratory insertion step, that is the energy difference between the octahedral complexes and the thermodynamic products, the pure QM calculations on the full systems predict methyl migration to be clearly exothermic for the **P,P-Ph** and **P,S-Ph** systems, and slightly exothermic for the **2P-Et** system. This is consistent with the experimental trends that the reaction goes to completion and gives a stable isolable acetyl product in the case of the **P,P-Ph** and **P,S-Ph** systems, whereas CO pressure was necessary to trap the five-coordinated acetyl as an octahedral product in the case of the **2P-ET** system.

Conclusions

In this paper we have investigated the steric and electronic effects in the two main steps of rhodium-catalyzed carbonylation reactions. In particular, we have investigated the energetics of oxidative addition of CH_3I to several square-planar complexes, and we investigated in detail the CO insertion step. The main conclusions of this study can be summarized as follow:

(1) All the systems considered adopt a square-planar geometry prior to CH_3I oxidative addition. As regards the **P,S** and **P,N** based systems, the isomer in which the CO group is trans to the S or N atom is clearly favored relative to the geometry in which the CO group is trans to the P atom. As regards the unbridged **2P** based system, the favored geometry presents the two P atoms trans to each other.

(2) As regards the octahedral complexes after CH_3I oxidative addition, a comparison between the unsubstituted pure QM models and the real-size QM/MM models indicates that the energy gain due to CH_3I oxidative addition is reduced considerably by the steric pressure of the substituents on the ligand, while the substantially similar results obtained with the real-size QM/MM and full QM models indicate that electronic effects are not the only factor in determining the energetic of oxidative addition. The steric effects are more relevant for the Ph-substituted ligands, the **P,P-Ph** system in particular, since in the latter system the four Ph substituents are quite a bit closer to the added CH_3 and I ligands. Finally, as regards the P,P and P,S based systems, geometries in which the CO group is trans to the added CH_3 group are of substantially higher energy relative to the isomer in which the CO group is in the mean plane of the P,P or P,S based ligand. The only exception is the full QM **P,P-Ph** system, for which the two isomers are isoenergetic. Solvent effects slightly stabilize the octahedral complexes relative to the separated square-planar complexes and free CH_3I.

(3) A comparison between the unsubstituted pure QM models and the real-size QM/MM models indicates that the energy barrier of the CO insertion reaction is lowered in the presence of the Ph and Et substituents. This effect is related to a relief of the steric pressure on the complex, as the systems move from a six-coordinated octahedral geometry toward a five-coordinate square-pyramidal geometry. As regards electronic contributions, a comparison between the real-size QM/MM and full QM models indicates that the Ph and Et substituents have opposite effects. The Ph substituents lower the CO insertion barrier, whereas the Et substituents increase it. The energy barrier calculated for the **P,S-Ph** system is in rather good agreement with the experimental values, whereas that of the **P,P-Ph** system is somewhat underestimated. Inclusion of solvent effects with the continuum model utilized leads only to a slightly better agreement.

(4) For all the systems considered the thermodynamic product adopts a square-pyramidal geometry with the $C(O)CH_3$ group in the apical position. The release of steric pressure on the octahedral complexes is reflected in a more favored thermodynamics of the reaction on going from the pure QM models to the real-size QM/MM models. However, electronic effects clearly dominate the thermodynamics of the reaction, which becomes endergonic for the full QM **P,N-Ph** system. Solvent effects stabilize the various systems differently. When these effects are considered all the products result from lower energy with respect to the octahedral complexes, with the exception of the **P,N-Ph** system.

Acknowledgment. We are grateful to Prof. J. Luque, Universitat de Barcelona, for helpful comments on solvation effects and for test calculations with the PCM model, to Dr. A. Haynes, University of Sheffield, and to Dr. F. Ruffo, Università di Napoli, for very useful discussions. L.C. thanks CESCA (Centre de Supercomputació de Catalunya) for financial support, and the CIMCF of the Università Federico II of Napoli for technical support. M.S. thanks the Dirección General de Enseñanza Superior e Investigación Científica y Técnica (MEC-Spain), Grant PB98-0457-C02-01, for financial support, and the Departament d'Universitats, Recerca i Societat de la Informació of the Generalitat de Catalunya for financial support through the Distinguished University Research Promotion 2001.

Supporting Information Available: Cartesian coordinates of all the real-size full QM systems (PDF). This material is available free of charge via the Internet at http://pubs.acs.org.

JA016468Z

(61) Cubero, E.; Orozco, M.; Hobza, P.; Luque, F. J. *J. Phys. Chem. A* **1999**, *103*, 6394.